ACCEPTED FOR PUBLICATION IN *The Astrophysical Journal Letters*
Preprint typeset using LaTeX style emulateapj v. 6/22/04

THE SPIN TEMPERATURE AND 21CM BRIGHTNESS OF THE INTERGALACTIC MEDIUM IN THE PRE-REIONIZATION ERA

MICHAEL KUHLEN, PIERO MADAU, & RYAN MONTGOMERY
Department of Astronomy & Astrophysics, University of California, Santa Cruz, CA 95064
accepted for publication in The Astrophysical Journal Letters

ABSTRACT

We use numerical hydrodynamical simulations of early structure formation in a ΛCDM universe to investigate the spin temperature and 21cm brightness of the diffuse intergalactic medium (IGM) prior to the epoch of cosmic reionization, at $z \lesssim 20$. In the absence of any radiative heating, collisions between neutral hydrogen atoms can efficiently decouple the spin temperature from the CMB only in dense minihalos and filaments. Shock heated gas shines in emission, surrounded by cooler gas visible in absorption. In the case of a warm, mostly neutral IGM, produced here by X-ray emission from an early miniquasar, the 21cm signal is strongly enhanced. Even slightly overdense filaments now shine in emission against the CMB, possibly allowing future radio arrays to probe the distribution of neutral hydrogen before reionization.

Subject headings: cosmology: theory – diffuse radiation – galaxies: evolution – intergalactic medium

1. INTRODUCTION

It has long been known that neutral hydrogen in the diffuse intergalactic medium (IGM) and in gravitationally collapsed structures may be directly detectable at frequencies corresponding to the redshifted 21cm line (Field 1959; Sunyaev & Zel'dovich 1975; Hogan & Rees 1979). The emission or absorption of 21cm photons from neutral gas is governed by the spin temperature T_S, defined as $n_1/n_0 = 3\exp(-T_*/T_S)$. Here n_0 and n_1 are the number densities of atoms in the singlet and triplet $n = 1$ hyperfine levels, and $T_* = 0.068\,\mathrm{K}$ is the temperature corresponding to the energy difference between the levels. To produce an absorption or emission signature against the cosmic microwave background (CMB), the spin temperature must differ from the temperature of the CMB, $T_{\rm CMB} = 2.73\,(1+z)\,\mathrm{K}$. At $30 \lesssim z \lesssim 200$, prior to the appearance of nonlinear baryonic objects, the IGM cools adiabatically faster than the CMB, spin-exchange collisions between hydrogen atoms couple T_S to the kinetic temperature T_K of the cold gas, and cosmic hydrogen can be observed in absorption (Scott & Rees 1990; Loeb & Zaldarriaga 2004). At lower redshifts, the Hubble expansion rarefies the gas and makes collisions inefficient: the spin states go into equilibrium with the radiation, and as T_S approaches $T_{\rm CMB}$ the 21cm signal diminishes. It is the first luminous sources that make uncollapsed gas in the universe shine again in 21cm, by mixing the spin states either via Lyα scattering or via enhanced free electron-atom collisions (e.g. Madau et al. 1997, hereafter MMR; Tozzi et al. 2000; Ciardi & Madau 2003; Gnedin & Shaver 2004; Nusser 2005).

While the atomic physics of the 21cm transition is well understood in the cosmological context, exact calculations of the radio signal expected during the era between the collapse of the first baryonic structures and the epoch of complete reionization have been difficult to obtain. This is because the "21cm radiation efficiency" depends on spin temperature, gas overdensity, hydrogen neutral fraction, and line-of-sight peculiar velocity (e.g. MMR; Bharadwaj & Ali 2004). When $T_S = T_K$, the visibility of the IGM at 21cm revolves around the quantity $(T_K - T_{\rm CMB})/T_K$. If $T_K < T_{\rm CMB}$, the IGM will appear in absorption against the CMB; in the opposite case it will appear in emission. To determine the kinetic temperature of the IGM during the formation of the first sources, one needs a careful treatment of the relevant heating mechanisms such as photoionization and shock heating. In addition to the signal produced by the "cosmic web", minihalos with virial temperatures of a few thousand kelvins form in abundance at high redshift, and are sufficiently hot and dense to emit collisionally-excited 21 cm radiation (Iliev et al. 2002).

In this *Letter*, we use fully 3D Eulerian cosmological hydrodynamical simulations of early structure formation to make detailed predictions of the thermal history, spin temperature, and 21cm brightness of neutral hydrogen in the pre-reionization era at $z \lesssim 20$. The adaptive mesh refinement (AMR) technique allows us to resolve, with progressively finer resolution, the radio signal expected from the densest parts of the IGM and from minihalos, and study the impact on 21cm spectral features of sources of X-ray radiation that may start shining before a univeral Lyα and Lyman-continuum background is actually established.

2. SPIN-KINETIC TEMPERATURE COUPLING

In the quasi-static approximation for the populations of the hyperfine levels, and in the absence of radio sources, the H I spin temperature at a given redshift is a weighted mean between T_K and $T_{\rm CMB}$,

$$T_S = \frac{T_* + T_{\rm CMB} + yT_K}{1+y}. \quad (1)$$

The coupling efficiency y is the sum of three terms,

$$y = \frac{T_*}{AT_K}\,(C_{\rm H} + C_e + C_p), \quad (2)$$

where $A = 2.85 \times 10^{-15}\,\mathrm{s}^{-1}$ is the spontaneous emission rate and $C_{\rm H}$, C_e, and C_p are the de-excitation rates of the triplet due to collisions with neutral atoms, electrons, and protons. A fourth term must be added in the

Electronic address: mqk@ucolick.org

presence of ambient Lyα radiation, as intermediate transitions to the $2p$ level can mix the spin states and couple T_S to T_K, the "Wouthuysen-Field" effect (Wouthuysen 1952; Field 1958; Hirata 2005).

The H-H collision term can be written as $C_{\rm H} = n_{\rm H}\kappa$, where κ is the effective single-atom rate coefficient recently tabulated by Zygelman (2005) for temperatures in the range $1 < T_K < 300\,{\rm K}$. For $300 < T_K < 1000$ K we have used the values tabulated by Allison & Dalgarno (1969) multiplied by a factor of 4/3 (as recommended by Zygelman 2005). These rates can be fitted by a simple function, $\kappa = 3.1\times10^{-11}\,T_K^{0.357}\exp(-32/T_K)\,{\rm cm^3\ s^{-1}}$, which is very accurate (to $< 0.5\%$) in the range $10 < T_K < 10^3$ K. This fit also extrapolates well to the $T_K = 3000\,{\rm K}$ and $T_K = 10^4\,{\rm K}$ coefficients ($\times 4/3$) listed in Field (1958). For the e-H collision term, $C_e = n_e\gamma_e$, we have used the functional fit of Liszt (2001) to the downward rates of Smith (1966), $\log(\gamma_e/{\rm cm^3\,s^{-1}}) = -9.607 + 0.5\log(T_K)\exp[-(\log T_K)^{4.5}/1800]$ for $T_K \le 10^4\,{\rm K}$, and $\gamma_e(T_K > 10^4\,{\rm K}) = \gamma_e(10^4\,{\rm K})$. The rate coefficient for proton de-excitation is just 3.2 times larger than that for neutral atoms at $T_K > 30\,{\rm K}$ (Smith 1966). We have used $\gamma_p = 3.2\,\kappa$ (with $C_p = n_p\gamma_p$): excitation by protons is typically unimportant as it is much weaker than that by electrons at the same temperature. In the absence of Lyα pumping, to unlock the spin temperature of a neutral medium with $T_K = 500\,{\rm K}$ from the CMB requires a collision rate $C_{\rm H} > AT_{\rm CMB}/T_*$, or a baryon overdensity $\delta_b > 5\,[(1+z)/20]^{-2}$. Not only dense gas within virialized minihalos but also intergalactic filamentary structure heated by adiabatic compression or shock heating may then be observable in 21cm emission. We shall see in the next sections how a population of "miniquasars" turning on at early stages (e.g. Madau et al. 2004; Ricotti et al. 2005) will make even the low-density IGM visible in 21cm emission as structure develops in the pre-reionization era.

3. NUMERICAL SIMULATIONS

The simulations have been performed using a modified version of ENZO, an AMR, grid-based hybrid (hydro+N-body) cosmological code developed by Bryan & Norman (see http://cosmos.ucsd.edu/enzo/). Details of the simulation setup are discussed in Kuhlen & Madau (2005, hereafter KM05). We follow the non-equilibrium, nine-species (H, H^+, H^-, e^-, He, He^+, He^{++}, H_2, and $H_2{}^+$) chemistry of primordial self-gravitating gas, including radiative losses from atomic and molecular line cooling, secondary ionizations and Compton heating by X-rays, and Compton cooling by the CMB. These simulations differ from those described in KM05 only in the use of the H_2 cooling function of Galli & Palla (1998) (instead of Lepp & Shull 1983) and of a new solver that couples the nine-species rate equations with the radiative gas cooling equations. The AMR is restricted to the inner 0.5 Mpc of a box of $L = 1$ Mpc (comoving) on a side: this region is allowed to dynamically refine to a total of 8 levels on a 128^3 top grid, resulting in a maximum resolution of 30 pc (comoving).[1] While the $L = 1$ Mpc box was selected to be a representative patch of the universe (with mean matter overdensity $\bar\delta = \rho/\bar\rho = 1$), the inner 0.5 Mpc region is characterized by $\bar\delta = 1.37$, corresponding to a $1.2-\sigma$ fluctuation.

The two-dimensional distribution of gas overdensity and spin temperature at $z = 17.5$ is shown in Figure 1 for a simulation with no radiation sources ("NoBH") and one ("PL") in which a miniquasar powered by a 150 $M_\odot$ black hole turns on at redshift 21 within a host halo of mass 2×10^6 $M_\odot$. The miniquasar shines at the Eddington rate and emits X-ray radiation with a power-law energy spectrum $\propto E^{-1}$ in the range $0.2-10\,{\rm keV}$. The black hole mass grows exponentially to 400 $M_\odot$ by $z = 17.5$. The color coding in this phase diagram indicates the fraction of the simulated volume at a given (δ_b, T_S). In both runs we have assumed no Lyα pumping, so that *the visibility of hydrogen at 21cm is entirely determined by collisions.* Only gas with neutral fraction $> 90\%$ is shown in the figure. The low-density IGM in the NoBH run lies on the yellow $T_S = T_{\rm CMB} = 50.4\,{\rm K}$ line: this is gas cooled by the Hubble expansion to $T_K \ll T_{\rm CMB}$ that cannot unlock its spin states from the CMB and therefore remains invisible. At overdensities between a few and ~ 200, H-H collisions become efficient and adiabatic compression and shocks from structure formation heats up the medium well above the radiation temperature. The coupling coefficient at this epoch is $y \sim \delta_b T_K^{-0.64}$: gas in this regime has $T_{\rm CMB} < T_S \sim yT_K < T_K$ and appears in *emission* against the CMB (red and green swath). Some residual hydrogen with overdensity up to a few tens, however, is still colder than the CMB, and is detectable in *absorption*. At higher densities, $y \gg 1$ and $T_S \to T_K$: the blue cooling branch follows the evolutionary tracks in the kinetic temperature-density plane of gas shock heated to virial values, $T_K = 2000-10^4\,{\rm K}$, which is subsequently cooling down to $\sim 100\,{\rm K}$ because of H_2 line emission. The volume and mass fractions of gas with $T_S > T_{\rm CMB}$ within the simulation box are $f_V = 0.002$ and $f_M = 0.068$, respectively. The latter is comparable to the amount of gas in the shocked phase estimated by Furlanetto & Loeb (2004, their fig. 8) using an extension of the Press-Schechter formalism.

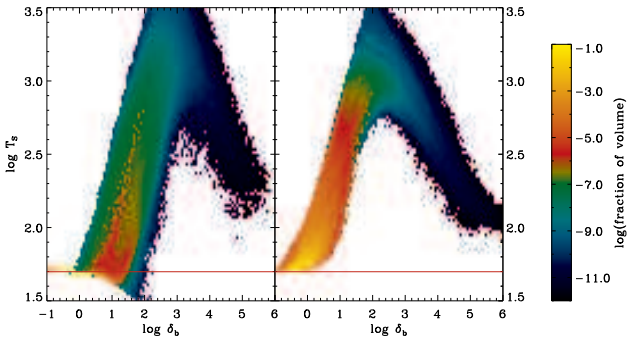

FIG. 1.— Two-dimensional distribution of spin temperature versus baryonic overdensity at $z = 17.5$. The color coding indicates the fraction of the simulated volume at a given (δ_b, T_S). *Left:* NoBH run. The volume and mass-averaged spin temperatures are 48.6 and 67.5 K, respectively. *Right:* PL run. Only gas with neutral fraction $> 90\%$ is shown in the figure. The volume and mass-averaged spin temperatures are 82.6 and 138.0 K, respectively. The red horizontal line marks the temperature of the CMB at that redshift.

The effect of the miniquasar on the spin temperature is clearly seen in the right panel of Figure 1. X-ray

[1] The DM density field is also sampled with 128^3 particles, leading to a mass resolution of $m_{\rm DM} = 2000\ M_\odot$. This ensures that halos above the cosmological Jeans mass are well resolved at $z < 20$.

radiation drives the volume-averaged temperature and electron fraction (x_e) within the simulation box from $(8\,\mathrm{K}, 1.4\times10^{-4})$ to $(2800\,\mathrm{K}, 0.03)$, therefore producing a warm, weakly ionized medium (KM05). The H-H collision term for spin exchange in the low-density IGM increases on the average by a factor $350^{0.36}\sim 8$, while the e-H collision term grows to $C_e\sim 0.5C_{\rm H}$. Gas with $(\delta_b, T_K, x_e) = (1, 2800\,\mathrm{K}, 0.03)$ has coupling efficiency $y = 0.008$, spin temperature $T_S = 73\,\mathrm{K} > T_{\rm CMB}$, and can now be detected in emission against the CMB. Within 150 comoving kpc from the source, the volume-averaged electron fraction rises above 10%, and e-H collisions dominates the coupling.

4. RADIO SIGNAL

A beam of 21cm radiation passing through a neutral hydrogen patch having optical depth τ and spin temperature T_S causes absorption and induces emission. In the comoving frame of the patch, the radiative transfer equation yields for the brightness temperature through the region: $T_b = T_{\rm CMB}e^{-\tau} + T_S(1-e^{-\tau})$. We have used our numerical simulations to perform 21cm radiation transport calculations, including the effect of peculiar velocities and local changes in spin temperature, gas density, and neutral hydrogen fraction, as follows. The equation of radiative transfer has been discretized according to

$$T_{b,\nu_0} = T_{\rm CMB}\, e^{-\sum_i \Delta\tau^i_{\nu_0}} + \sum_i T^i_S \Delta\tau^i_{\nu_0} e^{-\sum_j \Delta\tau^j_{\nu_0}}, \quad (3)$$

where T^i_S is the spin temperature of the $i^{\rm th}$ cell and ν_0 is the line-center 21cm frequency as measured in the box plane where the miniquasar is located. The i-sums are over all cells along an orthogonal line-of-sight through the box, while the j-sum is over all cells in front of the $i^{\rm th}$ cell. The optical depth of a cell with H I column $N^i_{\rm HI}$ is then given by

$$\Delta\tau^i_{\nu_0} = \frac{3c^2 A N^i_{\rm HI}}{32\pi\nu_0^2}\,\phi(\Delta\nu)\frac{T_*}{T^i_S}, \quad (4)$$

where $\Delta\nu = \nu_0 v_i/c$ to account for the bulk motion associated with peculiar and Hubble flow velocities, and $\phi(\Delta\nu)$ is the normalized line profile. The total line-of-sight bulk velocity of the $i^{\rm th}$ cell relative to the miniquasar plane at proper distance r_i can be written as $v_i = v_{i,p} + H(z)r_i$, where $H(z) = H_0\,[\Omega_M(1+z)^3+\Omega_\Lambda]^{1/2}$. In our simulations the typical line-of-sight component of the peculiar motion dominates over the Hubble expansion on scales below 40 comoving kpc. The line profile is entirely determined by thermal broadening, so that $\phi(\Delta\nu) = (\Delta\nu_D\sqrt{\pi})^{-1}\exp[-(\Delta\nu/\Delta\nu_D)^2]$, where $\Delta\nu_D = \nu_0\sqrt{2kT_K/(m_pc^2)}$ is the Doppler width. The final step in the process is to propagate the 21cm radiation from the simulation box at redshift $z = 17.5$ to the Earth. Neglecting foreground emission and absorption, the observed flux at frequency $\nu_0/(1+z)$ can be simply expressed by the differential brightness temperature against the CMB as $\delta T_b = (T_b - T_{\rm CMB})(1+z)^{-1}$. We have calculated δT_b maps consisting of 1024^2 pixels, corresponding to an angular resolution of $\sim 0.01''$ and a frequency resolution of 21 Hz. The latter is three orders of magnitude smaller than the Hubble flow across the entire box. The resulting 21cm radio signal is shown in Figure 2 (lower panels), together with an image of the *projected* hydrogen spin temperature (upper panels): the latter highlights the abundance of structure within our simulation box on scales up to hundreds of kpc. Due to Hubble and peculiar velocity shifts not all of this structure contributes to the δT_b map. In the NoBH simulation, coherent features in the IGM can be discerned in emission ($T_S > T_{\rm CMB}$, $\delta T_b > 0$): this filamentary shock-heated structure is typically surrounded by mildly overdense gas that is still colder than the CMB and appears in absorption ($T_S < T_{\rm CMB}$, $\delta T_b < 0$). The covering factor of material with $\delta T_b \le -10$ mK is 1.7%, comparable to that of material with $\delta T_b \ge +10$ mK: only about 1% of the pixels are brighter than +40 mK. While low-density gas (black color in the left-lower panel) remains invisible against the CMB in the NoBH run, *the entire box glows in 21cm after being irradiated by X-rays.* The fraction of sky emitting with $\delta T_b > (+10, +20, +30, +50, +100)$ mK is now (0.57,0.31,0.19,0.1,0.035).

5. CONCLUSIONS

We have performed high-resolution AMR cosmological hydrodynamic simulations of early structure formation in a ΛCDM universe to investigate the spin temperature and 21cm brightness of the IGM prior to the epoch of cosmic reionization. In the adopted cosmology, the simulated box size corresponds to an angular scale $\Delta\theta = 0.32'\,(L/\mathrm{Mpc})$ at $z = 17.5$. We have not tried to match this scale to the resolution/sensitivity of planned low-frequency arrays such as *LOFAR*, *MWA*, *PAST*, and *SKA*. Rather, our main goal here was to locate and resolve some of the physics that determines the observability of 21cm spectral features in the pre-reionization era. We have shown that, even in the absence of external heating sources, spin exchange by H-H collisions can make filamentary structures in the IGM (heated by adiabatic compression or shock heating) observable in 21cm emission at redshifts $z \lesssim 20$. Some cold gas with overdensities in the range 5-100 is still detectable in absorption at a level of $\delta T_b \lesssim -10\,\mathrm{mK}$, with a signal that grows as T_S^{-1} and covers a few percent of the sky. X-ray radiation from miniquasars preheats the IGM to a few thousand kelvins and increases the electron fraction: this boosts both the H-H and the e-H collisional coupling between T_S and T_K, making even low-density gas visible in 21cm emission well before the universe is significantly reionized. Any absorption signal has disappeared, and as much as 30% of the sky is now shining with $\delta T_b \gtrsim +20\,\mathrm{mK}$. As pointed out by Nusser (2005), the enhanced e-H coupling makes the spin temperature very sensitive to the free-electron fraction: the latter is also a tracer of the H_2 molecular fraction in the IGM. Note that when $T_S \gg T_{\rm CMB}$, the radio signal saturates in emission. 21cm saturation can readily be inferred for the dark-blue and reddish portions of the upper-right image in Figure 2. The brightness temperature through these regions would then remain approximately the same even in the presence of background Lyα radiation above the "thermalization" value for efficient hyperfine level mixing (corresponding at these epochs to ~ 0.1 Lyα photons per hydrogen atom, MMR). Of course, in this case even the low-density IGM would be lit up at 21cm, and the overall contrast in the radio signal would actually decrease.

Our NoBH δT_b maps seem to be in qualitative agreement with the results of Ahn et al. (2005), exhibiting

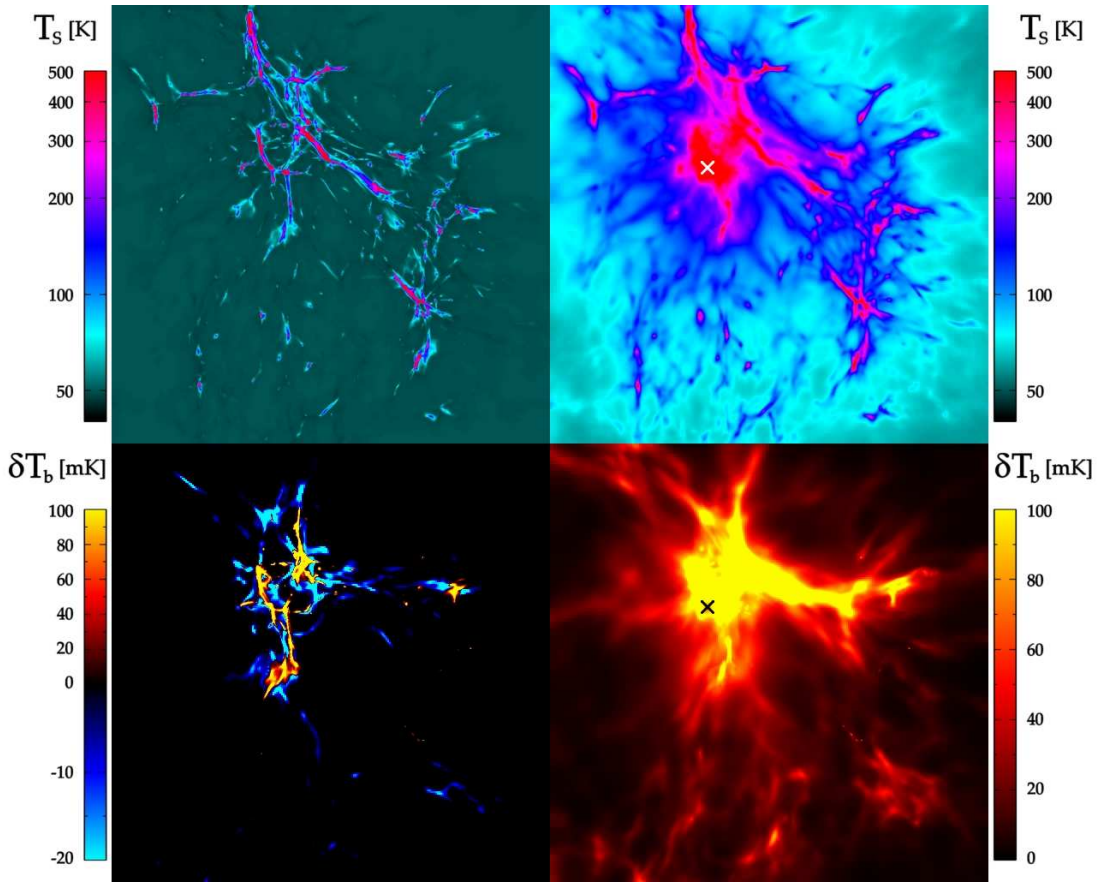

FIG. 2.— Projected (mass-weighted) spin temperature (*upper panels*, logarithmic scale) and 21cm differential brightness temperature (*lower panels*, composite linear scale) in a 0.5 Mpc simulation box for runs "NoBH" (*left*) and "PL" (*right*) at $z = 17.5$. The location of the miniquasar is indicated by crosses in the right panels.

both emission from minihalos and dense filaments and absorption from the cold IGM. Gas belonging to virialized minihalos (i.e. having baryonic overdensity $\delta_b > 70$, see KM05) contributes about 60% of the total emission signal while most of the absorbing signal (light blue color in the left-lower panel of Fig. 2) is due to gas with $\delta_b \lesssim 10$ still left below $T_{\rm CMB}$ by adiabatic heating. In the PL case instead, the signal is entirely in emission and is dominated by the warm, mostly neutral, diffuse IGM. Finally, we point out that, on the simulated scales, we find little evidence for a systematic enhancement of the radio signal due to velocity compression from baryonic infall (Barkana & Loeb 2005). Regions that are able to collisionally decouple their spin temperature from the CMB are non-linear density perturbations, for which redshift-space smearing ("fingers of god") outweighs the enhancement from the Kaiser effect. Peculiar velocities do, however, Doppler shift features into and out of the δT_b maps. We are running a suite of hydrodynamic simulations in larger cosmological volumes, which will allow predictions at the spatial and spectral resolution of future planned radio arrays.

Support for this work was provided by NASA grants NAG5-11513 and NNG04GK85G, and by NSF grants AST-0205738 (P.M.). All computations were performed on NASA's Project Columbia supercomputer system.

REFERENCES

Ahn K., Shapiro, P. R., Alvarez, M. A., Iliev, I. T., Martel, H., & Ryu, D. 2005, NewAR, in press (astro-ph/0509651)
Allison, A. C., & Dalgarno, A. 1969, ApJ, 158, 423
Barkana, R., & Loeb, A. 2005, ApJ, 624, L65
Bharadwaj, S., & Ali, S. S. 2004, MNRAS, 352, 142
Ciardi, B., & Madau, P. 2003, ApJ, 596, 1
Field, G. B. 1958, Proc. IRE, 46, 240
Field, G. B. 1959, ApJ, 129, 525
Furlanetto, S. R., & Loeb, A. 2004, MNRAS, 611, 642
Galli, D., & Palla, F. 1998, A&A, 335, 403
Gnedin, N. Y., & Shaver, P. A. 2004, ApJ, 608, 611
Hirata, C. M. 2005, MNRAS, submitted (astro-ph/0507102)
Hogan, C. J., & Rees, M. J. 1979, MNRAS, 188, 791
Iliev, I. T., Shapiro, P. R., Ferrara, A., & Martel, H. 2002, ApJ, 572, L123
Kuhlen, M., & Madau, P. 2005, MNRAS, 363, 1069
Lepp, S., & Shull, J. M. 1983, ApJ, 270, 578
Liszt, H. 2001, A&A, 371, 698
Loeb, A., & Zaldarriaga, M. 2004, PhRvL, 92, 211301
Madau, P., Meiksin, A., & Rees, M. J. 1997, ApJ, 475, 492 (MMR)
Madau, P., Rees, M. J., Volonteri, M., Haardt, F., & Oh, S. P. 2004, ApJ, 604, 484
Nusser, A. 2005, MNRAS, 359, 183
Ricotti, M., Ostriker, J. P., & Gnedin, N. Y. 2005, MNRAS, 357, 207
Scott, D., & Rees, M. J. 1990, MNRAS, 247, 510

Smith, F. J. 1966, P&SS, 14, 929
Sunyaev, R. A., & Zel'dovich, Y. B. 1975, MNRAS, 171, 375
Tozzi, P., Madau, P., Meiksin, A., & Rees, M. J. 2000, ApJ, 528, 597
Wouthuysen, S. A. 1952, AJ, 57, 31
Zygelman, B. 2005, ApJ, 622, 1356